Figure 1: PTCH1 gene suppression leads to increased GLI1 activity

[**A**] NEB1-shPTCH1 cells show reduced PTCH1 and increased GLI1 protein expression, both PTCH1-C20 and GLI1-H300 antibodies display a nuclear staining pattern. [**B**] Suppression of PTCH1 reduces mRNA expression of SHH and IHH ligands with increased GLI1 and SMO but no significant change in GLI2 levels. [**C**] NEB1-shPTCH1 transfected with a 6x GLI binding site Firefly Luciferase reporter construct (6xGLI-BS-Firefly) and EGFP as a transfection control, confirm increased GLI1 activity based on a 3-fold increase in Luciferase mRNA expression. [**D**] Ectopic expression of the PTCH1B isoform (shRNA targets exon 24 beyond the STOP codon in exon 23) suppressed the increased GLI1 mRNA expression in NEB1-shPTCH1 cells. [**E**] NEB1-shPTCH1 cells form densely packed colonies similar in appearance to nodular or micronodular BCC tumours. [**F**] Due to tight packing of NEB1-shPTCH1 cells, the size of the nuclei appear smaller with a greater average number of nucleoli present (average taken from 50 cells). *P≤0.05 and **P≤0.01 (as calculated by Student's *t* test), error bars represent standard deviation, n=6.
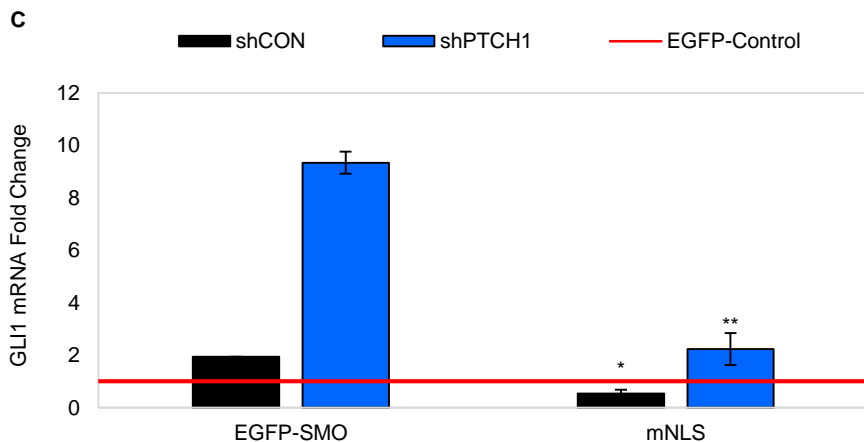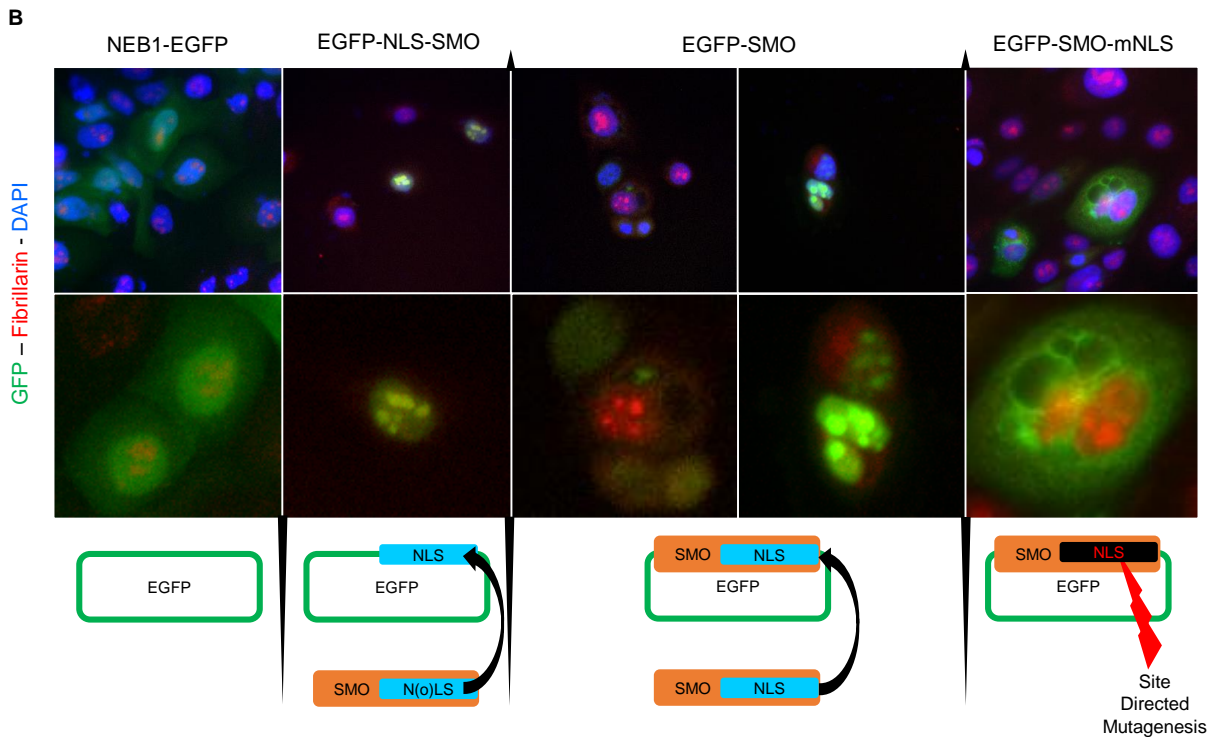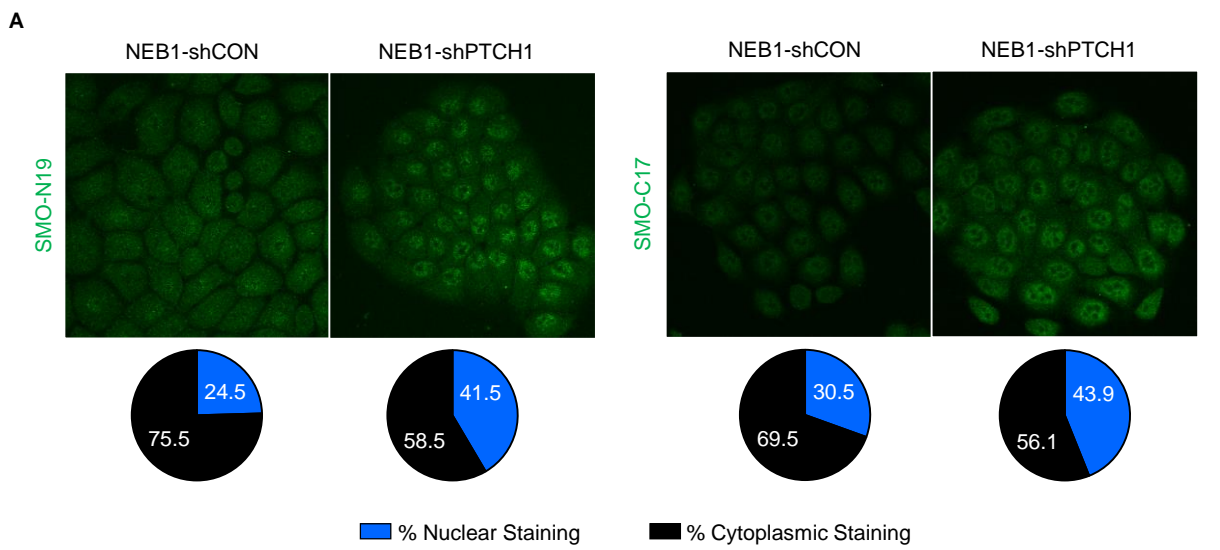
Figure 2: GLI1 is activated by nuclear SMO

[**A**] Staining using two SMO antibodies (N and C terminal protein) revealed distinct nuclear localisation of SMO in shPTCH1 cells with a higher percentage of nuclear SMO in shPTCH1 cells (calculated by ImageJ, n=20). [**B**] NEB1 cells transfected with EFP containing the predicted N(o)LS sequence from SMO directs GFP to the nucleolus (Supplementary C). EGFP-SMO fusion protein is expressed in both the nucleus and nucleolus and by mutating the N(o)LS, nucleolar GFP expression is lost and the protein is retained in the cytoplasm. [**C**] shCON cells and to a greater extent shPTCH1 cells transfected with EGFP-SMO show upregulation of GLI1 mRNA expression that is then reduced to below basal levels upon mutation of N(o)LS sequences. *P≤0.05 and **P≤0.01 (as calculated by Student's *t* test), error bars represent standard deviation, n=6.
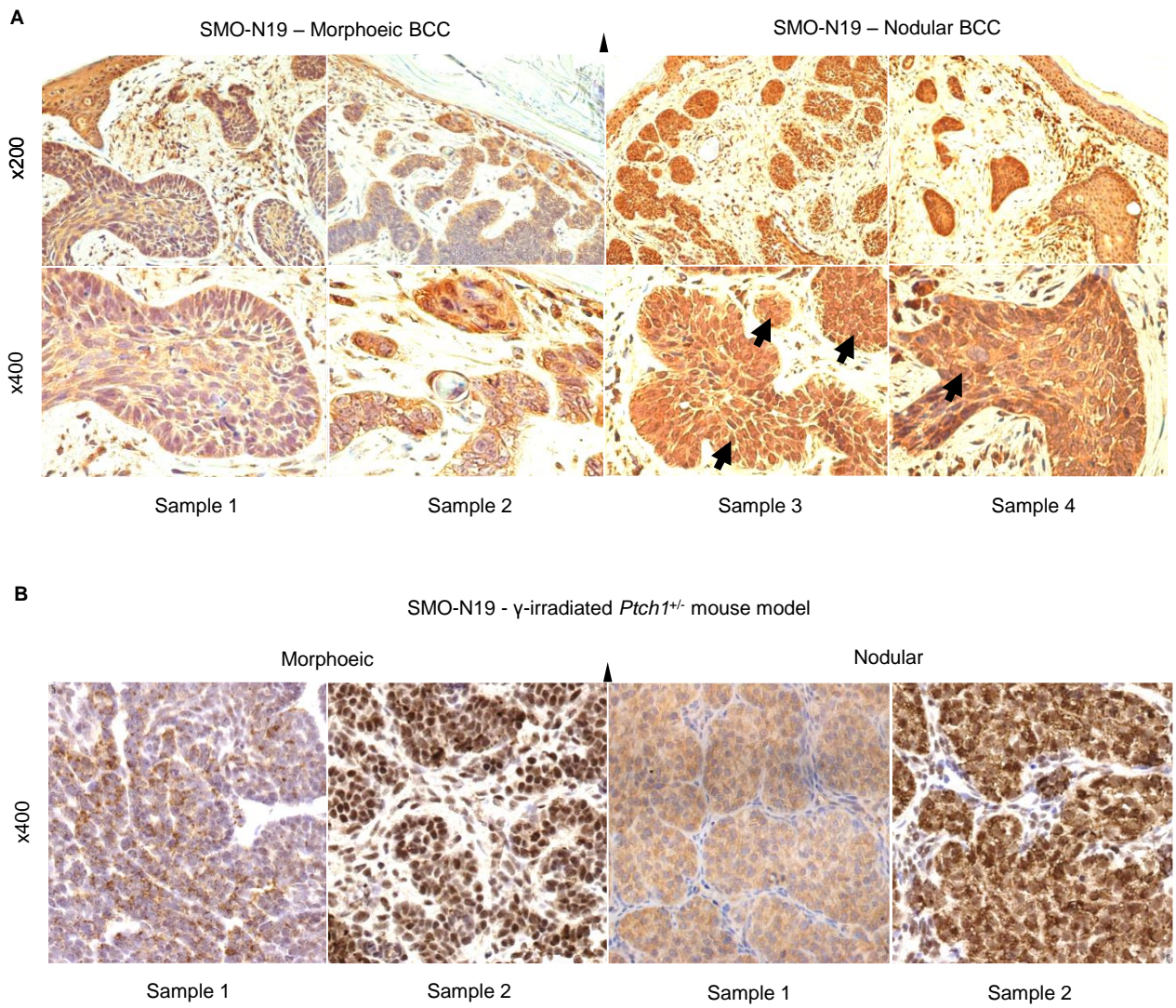
Figure 3: Nuclear SMO expression is observed in mammalian skin and BCCs
[**A**] SMO-N19 staining of human morphoeic BCCs show cytoplasmic expression and variable staining intensities while nodular BCCs also express cytoplasmic SMO; certain tumour nodules also express nuclear SMO protein (marked by arrows). [**B**] Mouse BCC tumours derived from *Ptch1*^{+/-} γ-irradiated mice show distinct nuclear SMO expression although there is heterogeneity between tumours.
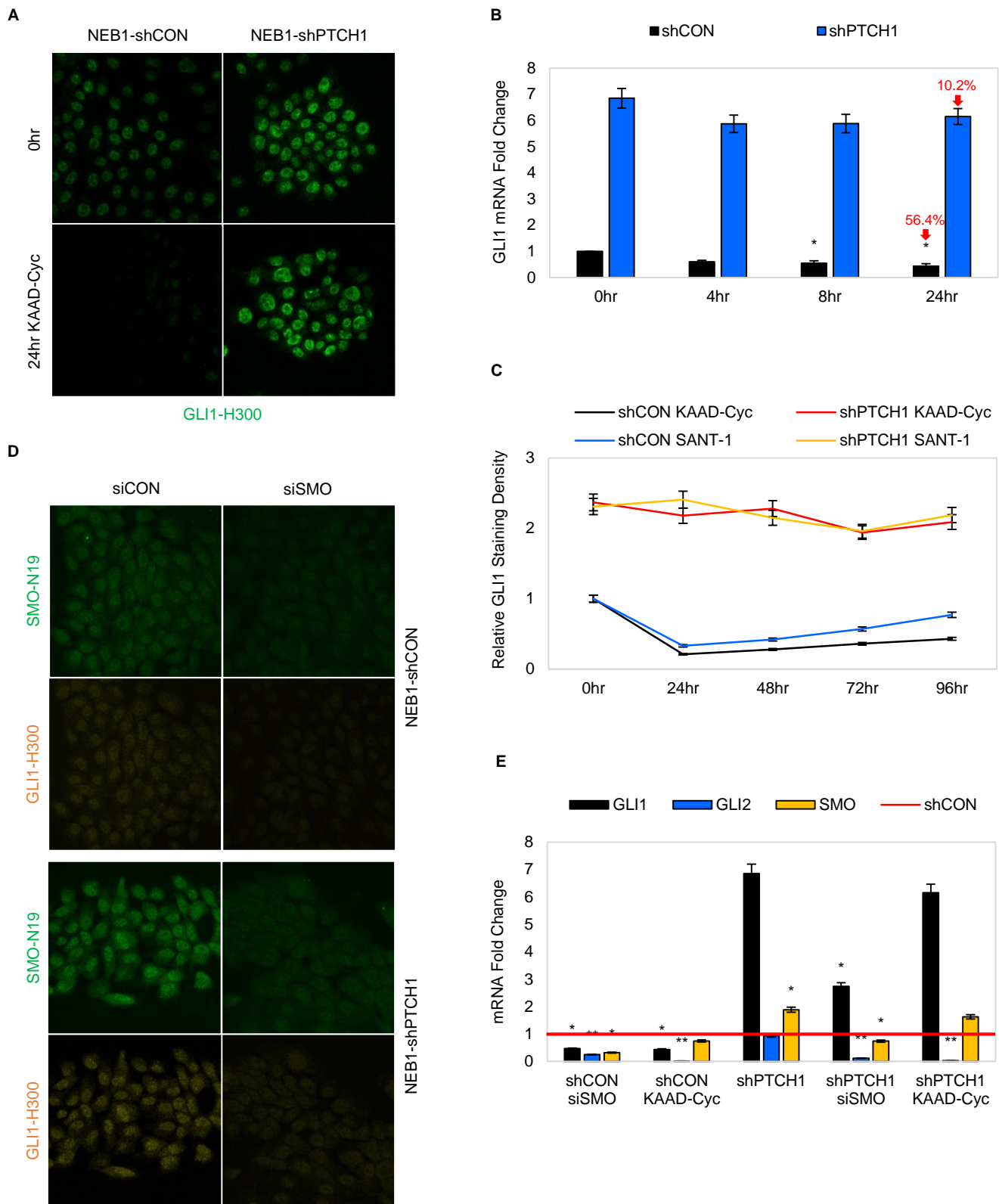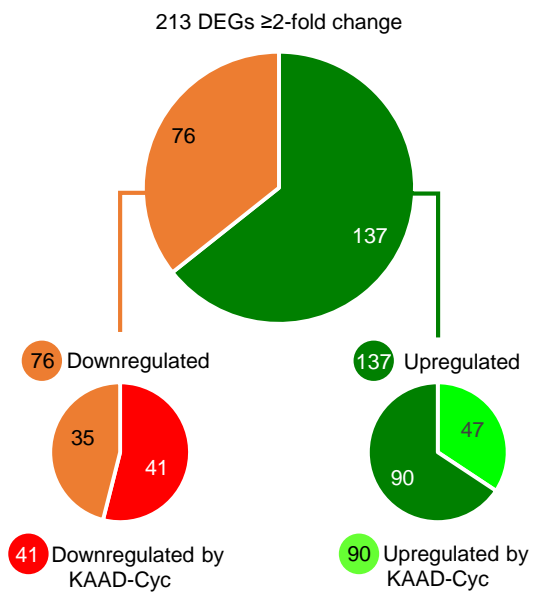
Figure 4: PTCH1-suppressed cells are unresponsive to anti-SMO inhibitors
24 hours of 100 nM KAAD-Cyc is able to suppress GLI1 [**A**] protein and [**B**] mRNA expression in NEB1-shCON cells however, NEB1-shPTCH1 cells show no GLI1 reduction. [**C**] The same lack of response in NEB1-shPTCH1 cells was seen with 100 nM SANT-1, also with extended treatment up to 96 hours where GLI1 protein remained constant. [**D**] Although shPTCH1 cells did not respond to SMO inhibitors, SMO siRNA (siSMO) did suppress GLI1 protein expression compared to control siRNA (siCON) suggesting that SMO is required for GLI1 signalling. [**E**] qPCR confirms that GLI1 expression is reduced by siSMO but not KAAD-Cyc in shPTCH1 cells while GLI2 expression is suppressed by both siSMO and KAAD-Cyc. *P≤0.05 and **P≤0.01 (as calculated by Student's *t* test), error bars represent standard deviation, n=6.

Table 1: List of top and bottom DEGs

Gene	Fold Change vs. shCON shPTCH1	KAAD-CYC	Gene	Fold Change vs. shCON shPTCH1	KAAD-CYC	Gene	Fold Change vs. shCON shPTCH1	KAAD-CYC
MMP7	9.4698	4.9019	SPOCK1	2.3674	2.8024	PPP1R16B	-2.0046	-2.0232
SCGB1A1	9.1472	6.0769	SERPINA1	2.3565	2.0658	FAM174B	-2.0232	-2.1785
CXCL10	8.2059	3.8459	TNC	2.3565	2.0562	EPGN	-2.0326	-2.0232
PTGIS	7.0453	4.9474	F8	2.3511	2.1835	CHAC1	-2.0373	-4.1030
ANKRD1	6.4681	6.3938	EVI2B	2.3349	2.0093	MAP2K6	-2.0373	-2.0093
THY1	6.3496	7.2267	F2RL1	2.3295	2.4909	PAIP2B	-2.0467	-1.7573
NNMT	5.5416	5.1814	GPNMB	2.3241	1.6740	PAG1	-2.0467	-1.7736
SRPX	5.0397	4.8793	ZFP57	2.3187	1.7777	NDUFAF1	-2.0610	-2.0093
ESX1	4.9818	4.9019	ANXA6	2.3134	1.9453	RNASE4	-2.0610	-1.8921
CXCL11	4.8906	5.2198	IGFBP7	2.3027	2.4396	ZNF585B	-2.0705	-2.2658
ADAM19	4.8456	5.1456	LIPG	2.2868	2.3950	UPK1B	-2.0753	-1.9816
IL7R	4.8456	4.2281	CERCAM	2.2710	2.3080	EDNRA	-2.0898	-1.2138
GPRC5B	4.7349	4.1892	HTR1D	2.2710	1.7777	SLC6A14	-2.0994	-2.2974
FAM20C	4.5315	4.1315	ARSI	2.2449	2.0139	ZNF214	-2.1140	-2.0232
SAA1	4.4076	3.5064	ARRB1	2.2243	2.2658	GPR1	-2.1189	-2.9622
LAPTM5	4.2477	4.0652	EBI3	2.2140	1.7736	PARP16	-2.1238	-2.5787
MMP2	4.1315	3.8637	MICB	2.2140	2.2763	SLC7A11	-2.1238	-3.3674
LIFR	3.9908	4.8232	DOCK11	2.2140	2.4737	ZNF750	-2.1337	-3.3134
CYP24A1	3.8548	3.8018	ST6GAL1	2.2089	1.9274	FAM174A	-2.1337	-1.8575
CFB	3.8194	2.6329	CCL20	2.2089	2.2501	ENPP5	-2.1485	-1.9453
ALDH2	3.7842	3.9908	ENG	2.2089	2.4061	SEL1L	-2.1585	-2.8812
MCAM	3.7581	4.3369	TOX2	2.2038	2.1092	SULT2B1	-2.1685	-3.3674
APOBEC3G	3.6050	2.4284	MMP9	2.1987	2.3187	TMEM45B	-2.1785	-2.2397
VIM	3.5718	3.4027	SAA2	2.1987	2.1485	C7orf31	-2.1835	-2.4005
SLCO2A1	3.5718	3.7494	REPS2	2.1785	1.9185	STARD5	-2.1936	-3.1602
FAP	3.4661	3.5145	GRAMD1B	2.1735	2.7069	FBP1	-2.2038	-1.9588
TRIM31	3.4502	1.8067	HCP5	2.1485	1.9230	ASNS	-2.2191	-3.0175
APOD	3.3792	2.5967	NFIB	2.1485	2.2346	ACADSB	-2.2243	-1.8319
PMEPA1	3.3714	3.7321	INSIG1	2.1435	2.0753	SLC19A3	-2.2346	-1.7736
SERPINA3	3.3636	2.3565	CKB	2.1386	2.1287	GJB6	-2.2605	-1.7613
SIRPA	3.3636	3.9282	KLK10	2.1386	1.9588	HMGN5	-2.2395	-2.3134
INHBA	3.3173	3.3173	RND1	2.1337	1.5511	ANKRD22	-2.3839	-2.7766
TGFB2	3.2868	3.3173	F2R	2.1337	1.9908	RPS6KA6	-2.4061	-1.8319
IFITM1	3.2716	2.9690	TNFRSF6B	2.1140	2.1092	SCNN1B	-2.4116	-2.9147
HLA-B	3.2565	2.9690	CEACAM1	2.1043	1.7132	MTSS1	-2.4340	-2.3674
ATP8A2	3.0314	2.8812	LONRF3	2.1043	2.0753	BMP7	-2.4566	-2.3080
SLC2A12	3.0175	3.3295	SDC3	2.1043	2.2658	WASF3	-2.4852	-3.5257
LOXL2	2.9417	3.2191	DGAT2	2.0994	2.7007	SCNN1G	-2.5024	-2.4680
RNASE7	2.9012	1.9141	LIF	2.0898	2.2089	LRRC6	-2.5082	-2.4909
LPXN	2.8613	2.5550	LXN	2.0801	1.4109	UPK3B	-2.5374	-2.5491
C15orf48	2.8613	2.4396	NRCAM	2.0753	1.1238	MANEA	-2.5491	-2.3187
TRIM22	2.8415	2.4737	CARD17	2.0753	1.3724	SPRR1B	-2.5907	-2.7702
IL32	2.8219	2.2397	SERPING1	2.0753	2.0139	FAM63B	-2.6268	-2.2763
CDH2	2.7830	3.7668	PTGS1	2.0705	2.0420	POF1B	-2.6635	-2.4967
GBP1	2.7574	4.2228	CST6	2.0705	2.4116	IGFBP2	-2.6759	-2.9828
PLOD2	2.7447	3.3173	PDCD1LG2	2.0515	2.4680	CAPNS2	-2.7069	-3.1675
ZNF114	2.7258	2.7321	PPP2R2C	2.0515	2.2605	TGM1	-2.7447	-3.3636
ATP6V0D2	2.7195	2.0515	MX1	2.0515	1.7859	SEC11C	-2.7638	-2.8945
SPATA18	2.6945	2.4909	PAPSS2	2.0515	2.4852	C1orf21	-2.8024	-3.3457
GULP1	2.6945	2.2763	PTGER2	2.0420	2.0898	PPFIBP2	-2.9079	-2.9759
DOCK10	2.6512	2.6945	TEAD2	2.0420	2.1685	CXCR7	-2.9485	-3.4502
ACTBL2	2.6512	2.4340	SERPINB4	2.0420	1.6058	TCF7L1	-2.9485	-3.3716
CYGB	2.6512	2.9622	CSF1	2.0373	1.8489	SPRR1A	-3.0105	-3.4343
MMD	2.6208	2.7574	SAA4	2.0373	1.5728	WDR17	-3.0175	-2.4623
MDK	2.6147	2.4623	APOC1	2.0279	2.0279	ANKFN1	-3.0667	-2.8415
CST2	2.6147	2.4116	CD14	2.0232	1.9725	KRT15	-3.1023	-4.4795
MYB	2.6087	2.4453	KMO	2.0139	1.4241	SERPINB13	-3.2266	-2.6575
MUC4	2.6087	2.0705	FAM172B	2.0046	1.8747	SH3BGRL	-3.2415	-3.3636
PLAU	2.5907	2.4623	SHC3	2.0046	2.0610	AGR2	-3.3173	-5.8835
QPRT	2.5787	2.7321	IL24	2.0000	1.5728	SPRR3	-3.3250	-4.7568
PLAT	2.5669	2.7447	TLR6	2.0000	1.4845	ZNF165	-3.4661	-5.3641
IRAK2	2.5609	2.2868				EPB41L4A	-3.4661	-3.5472
IDO1	2.5609	1.8532				SCD5	-3.4822	-3.4343
HSD17B2	2.5198	1.8108				AMOT	-3.6553	-3.4343
KRT81	2.5198	2.2294				SULT1E1	-3.7149	-5.2174
CTSS	2.4852	1.9453				KRT4	-3.8106	-4.7240
SNORA38B	2.4680	-1.1434				MCOLN3	-3.8282	-3.6893
CACNA2D1	2.4623	2.7959				H2AFY2	-3.9267	-3.8548
SLC41A2	2.4453	2.6451				PNLIPRP3	-4.3269	-6.0769
NA	2.4396	2.5082				CNTN1	-4.3469	-4.4795
ACSL5	2.4116	2.1287				MUC15	-4.3772	-3.7235
HEG1	2.4005	2.2140				KLHL13	-4.5525	-4.5842
SNAI1	2.4005	2.3241				LASS3	-5.8159	-5.7491
P2RY6	2.3950	2.3565				ARHGEF9	-8.8538	-7.9815
GLIPR1	2.3784	2.6635				C9orf125	-8.734	-8.0000
SERTAD4	2.3784	2.3950				FBN2	-10.1965	-10.0329

A 213 DEGs ≥2-fold change

76 — 137

76 Downregulated — 137 Upregulated

35 — 41 / 47 — 90

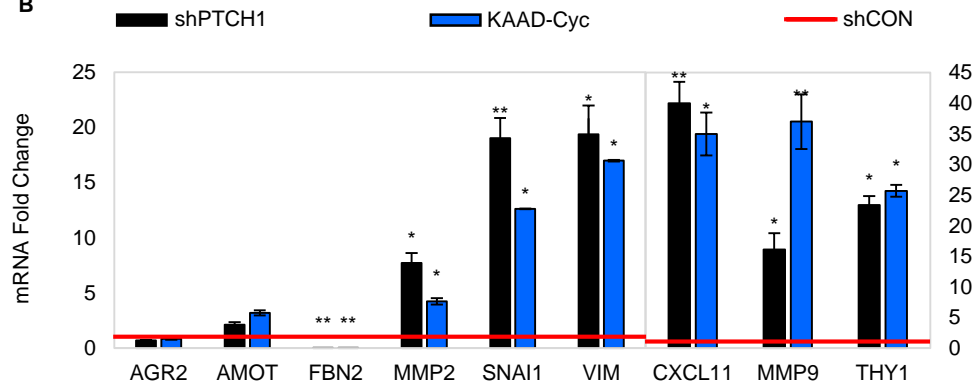41 Downregulated by KAAD-Cyc — 90 Upregulated by KAAD-Cyc

B

Figure 5: The global effects of PTCH1 suppression are largely insensitive to SMO inhibition
[**Table 1**] List of top and bottom DEGs (≥2 fold change, p>0.01) comparing NEB1-shPTCH1 and NEB1-shPTCH1 treated with 100 nM KAAD-Cyc to NEB1-shCON cells reveals various genes reported to be involved in BCC biology are differentially expressed. [**A**] Diagram of identified DEGs and the proportion of upregulated and downregulated genes further altered by KAAD-Cyc treatment. [**B**] qPCR on NEB1-shPTCH1 cells was performed to validate the results from the microarray with a number of cancer related genes all strongly upregulated in NEB1-shPTCH1 and also in cells treated with 100 nM KAAD-Cyc. *P≤0.05 and **P≤0.01 (as calculated by Student's *t* test), error bars represent standard deviation, n=6.

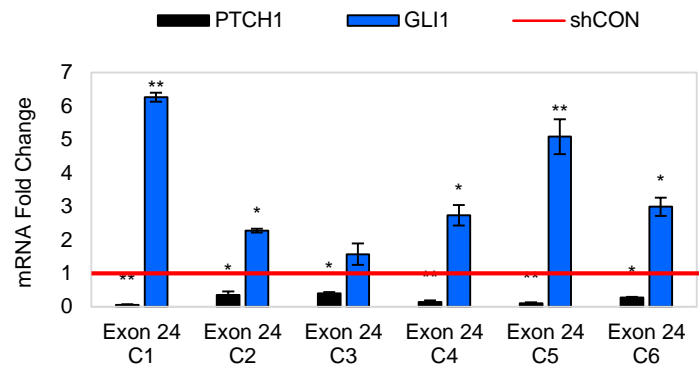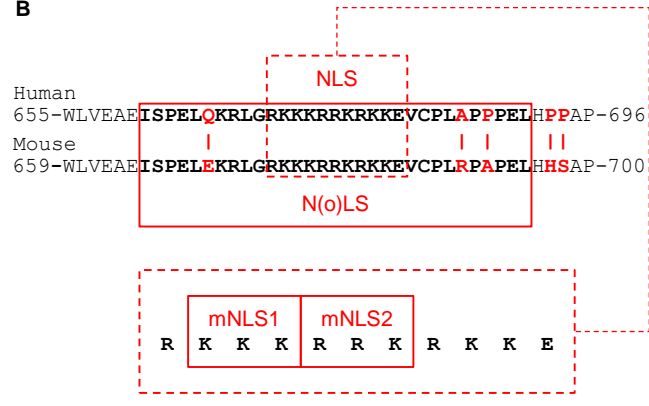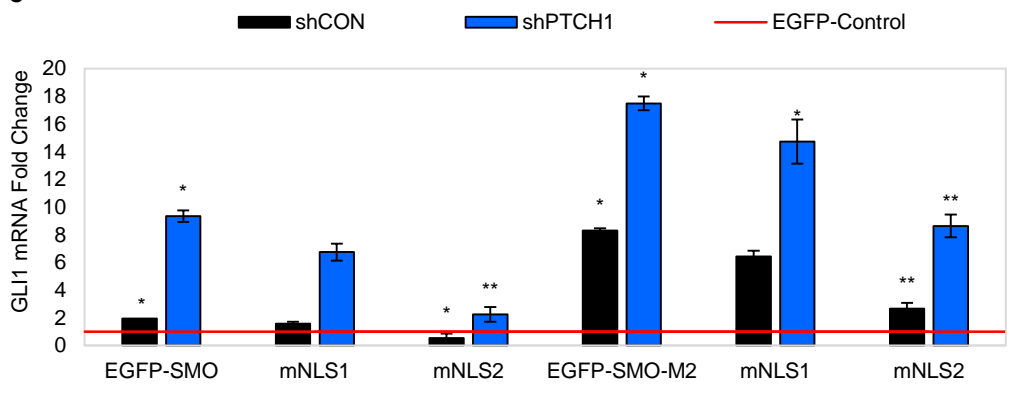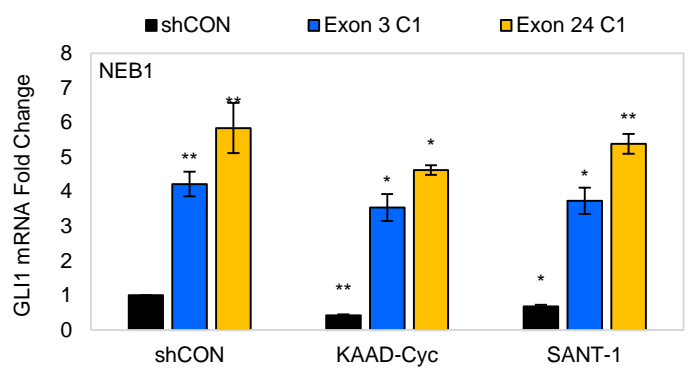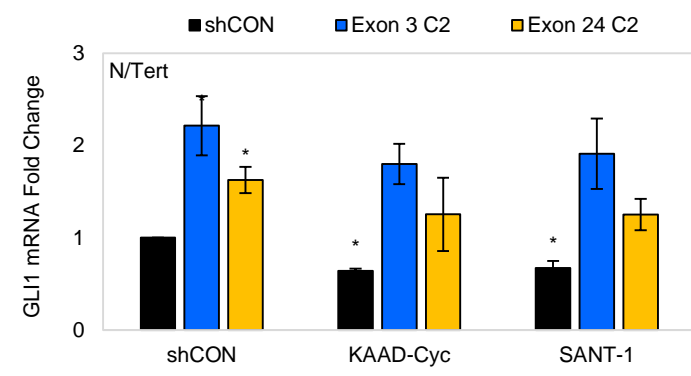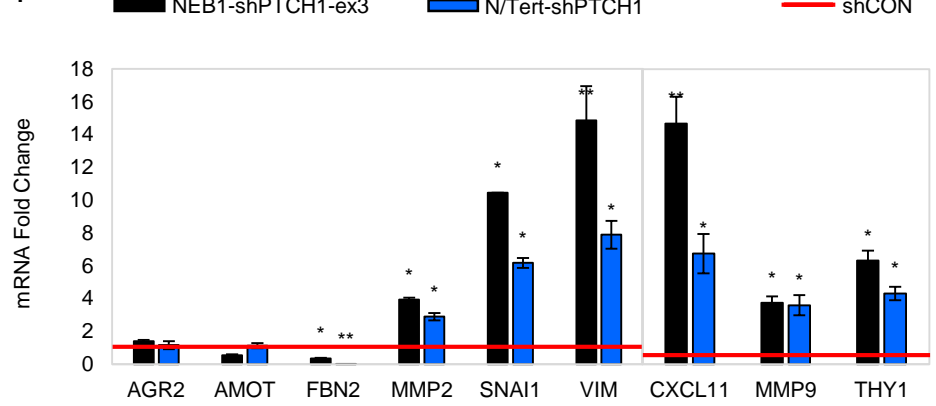**Table 1:** List of differentially expressed zinc-finger protein genes

Gene	Fold Change vs. shCON	
	shPTCH1	KAAD-CYC
ZNF114	2.7258	2.7321
ZFP57	2.3187	1.7777
ZNF555	-1.5655	-2.0000
ZNF391	-1.5263	-2.0046
ZNF804A	-1.7859	-2.1785
ZNF585B	-2.0705	-2.2658
ZNF214	-2.1140	-2.0232
ZNF750	-2.1337	-2.3134
ZNF165	-3.4661	-5.3641

Supplementary:

[**A**] Various exon 24 clones generated from heterogeneous populations of PTCH1 suppressed NEB1 cells show reduced PTCH1 and increased GLI1 mRNA expression. [**B**] Both human and mouse SMO protein sequences contain predicted nuclear and nucleolar localisation signals located within the C-terminal region, non-matching amino acids are highlighted in red. Site directed mutagenesis was employed to alter the N(o)LS by changing each amino acid to alanine for the mNLS construct, mNLS2 was used for Figures 2B and 2C. [**C**] NEB1-shCON cells and to a greater extent NEB1-shPTCH1 cells transfected with EGFP-SMO and EGFP-SMO-M2 show upregulation of GLI1 mRNA expression that is then reduced to below basal levels upon mutation of N(o)LS sequences, particularly mNLS2. qPCR analysis for GLI1 expression in [**D**] NEB1 and [**E**] N/Tert exon 3 and exon 24 shPTCH1 clones treated with both KAAD-Cyc and SANT-1 show all shPTCH1 clones are unresponsive to SMO pharmacological inhibitors. [**F**] qPCR on NEB1-shPTCH1 exon 3 clone and N/Tert-shPTCH1 cells to validate the results for cancer related genes obtained from the microarray analysis. [**Table 1**] List of differentially expressed zinc-finger protein genes. *P≤0.05 and **P≤0.01 (as calculated by Student's t test), error bars represent standard deviation, n=6.